Heterogeneous & Homogeneous & Bio- & Nano-

CHEMCATCHEM

CATALYSIS

Accepted Article

Title: Stabilization of Pd3−xIn1+x Polymorphs with Pd-like Crystal Structure and their Superior Performance as Catalysts for Semi-Hydrogenation of Alkynes

Authors: Shaun Kegan Johnston, Thomas A. Bryant, Jonathan Strong, Laura Lazzarini, Alex O. Ibhadon, and Maria Grazia Francesconi

To be cited as: *ChemCatChem* 10.1002/cctc.201900391

Link to VoR: http://dx.doi.org/10.1002/cctc.201900391

A Journal of

ChemPubSoc Europe

WILEY-VCH

www.chemcatchem.org

10.1002/cctc.201900391

Stabilization of $Pd_{3-x}In_{1+x}$ Polymorphs with Pd-like Crystal Structure and their Superior Performance as Catalysts for Semi-Hydrogenation of Alkynes

Shaun K. Johnston,[a] Thomas A. Bryant,[b] Jonathan Strong,[a] Laura Lazzarini,[c] Alex O. Ibhadon[d]* and M. Grazia Francesconi[a]*

[a] Department of Chemistry, University of Hull, Hull, HU6 7RX, UK.

[b] European Bioenergy Research Institute, Aston University, B4 7ET, UK.

[c] IMEM-CNR Parco Area delle Scienze 37/A, 43124 Parma, Italy.

[d] School of Engineering and Computer Science – Chemical Engineering, University of Hull, Hull, HU6 7RX, UK

Abstract

Selective hydrogenation (semi-hydrogenation) reactions of alkynes rely on Pd-based catalysts to provide the correct pathway to favour formation of double bonds and avoid full hydrogenation to single bonds. Here, we present the preparation and characterisation of "Pd_3In"/TiO_2 nanocatalysts, which show improved activity and selectivity compared to pure Pd catalysts, towards the liquid phase semi-hydrogenation of 2-methyl-3-butyn-2-ol (MBY) to 2-methyl-3-buten-2-ol (MBE), a fundamental step in the preparation of pharmaceuticals, and other industrially produced substances, as well as a model reaction for the semi-hydrogenation of alkynes.

For both the supported and unsupported "Pd_3In" alloys (later re-defined as $Pd_{3-x}In_{1+x}$), we stabilised two new cubic polymorphs with a Pd-like structure, instead of the tetragonal structure as reported so far in the literature. The stabilisation of these new polymorphs was made possible by using a solution-based synthesis and, thanks to the use of different solvents, the reaction was

carried out at different temperatures and the Pd/In ratio could be tuned. The same synthetic approach was adapted to prepare two "Pd_3In"/TiO_2 catalysts by adding the TiO_2 support to the reaction mixture, in a practical one-step, one-pot reaction. HREM and X-Ray maps show that the cubic crystal structure of "Pd_3In" is maintained when prepared in the presence of the support, however, the support seems to influence the Pd/In ratio.

1. Introduction

Hydrogenation reactions most commonly involve the addition of H_2 to a carbon-carbon multiple bond and constitute crucial steps in the synthesis of many fine chemicals including vitamins, pharmaceuticals, fragrances, cosmeceuticals and nutritional substances.[1,2]

The terms "semi-hydrogenation" or "selective hydrogenation" refer specifically to the partial hydrogenation of a C≡C triple bond (alkyne) to a C=C double bond (alkene), and avoiding full hydrogenation to a C-C single bond (alkane).

The semi-hydrogenation of 2-methyl-3-butyn-2-ol (MBY) to 2-methyl-3-buten-2-ol (MBE) (Figure 1) is an important starting reaction in industry and is widely used as a model substrate to screen for activity and selectivity of catalyst materials in semi-hydrogenation reactions.[3]

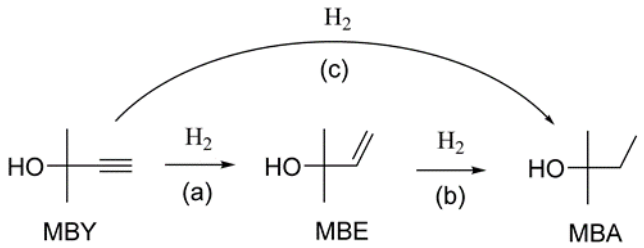

Figure 1. Reaction scheme of the hydrogenation of MBY to MBA. (MBY = 2-methyl-3-butyn-2-ol, MBE = 2-methyl-3-butene-2-ol and MBA = 2-methylbutan-2-ol.) For a selective semi-hydrogenation, steps (b) and (c) should be avoided.

To date the best heterogeneous catalysts for semi-hydrogenation reactions are Palladium-based catalysts, as they are very active and more selective than other platinum-group metals. However, their selectivity towards alkene products is still limited due to over-hydrogenation to alkanes and other side reactions such as dimerization and oligomerization reactions.[4,5] To overcome this drawback, a second metal (co-metal) is often added to Pd to increase the selectivity. The co-metal can be added to Pd metal as a surface poison, as is the case in the widely used Lindlar catalyst, in which Pb nanoparticles are added to Pd metal nanoparticles supported on $CaCO_3$ ($Pd/CaCO_3$).[6] However, the use of lead for catalyst modification is subject to increasing environmental concern, hence viable alternatives are required.[7]

Another route to add a co-metal to Pd metal is a chemical reaction between Pd metal and the co-metal to form a Pd-M alloy.

The reason for the enhancement of selectivity in a Pd-M alloy is not completely known, however two main factors have been identified. Firstly, an increase in selectivity can occur due to changes in the electronic structure of Pd brought on by the presence of an additional metal. The different electronic structure leads to a change in the relative adsorption energies of alkyne and alkene bonds, then resulting in a more favourable adsorption, hence hydrogenation of alkyne, while disfavouring the adsorption/hydrogenation of alkene species.[8] Secondly, alloy formation can reduce the number and size of active site ensembles due to "dilution" of Pd.[9] In fact, the addition of a second metal changes the coordination environment of Pd metal, which is then surrounded either by the co-metal atoms or by a mixture of co-metal and Pd atoms. Furthermore, in Pd-M compounds, the catalytically active Pd centres are, in general, farther apart than they are in Pd metal. This environment can inhibit secondary reactions that involve different functional groups, or neighbouring reactants to be adsorbed in close proximity to each other.

In 1984, the intermetallic compound Pd_3Pb was reported as a highly active and selective catalyst for semi hydrogenation of alkynes. Its selectivity was attributed to geometric effects related to its ordered crystal structure (cubic unit cell, $Pm\bar{3}m$, a = 4.035(1) Å) derived from the Pd crystal structure (cubic unit cell, $Fm\bar{3}m$, a = 3.867(3) Å), with Pb occupying the (0,0,0) positions and Pd occupying the (0, 0.5, 0.5) positions. In Pd metal, Pd is coordinated by 12 Pd atoms at a distance d = 2.744 Å, whereas in Pd_3Pb, Pd is coordinated by 8 Pd atoms and 4 Pb atoms, at an average distance d = 2.853 Å.[10,11]

Recently, we reported two catalysts Pd_3Sn/TiO_2 and Pd_3Sn/ZnO and compared their catalytic performance to Pd/TiO_2 and Pd/ZnO, all prepared following the same polyol-based synthesis method. All four catalysts showed high activity and selectivity for the selective hydrogenation of MBY to MBE in the liquid phase under identical conditions. However, Pd_3Sn/TiO_2 and Pd_3Sn/ZnO show selectivities significantly higher than that of the Pd catalysts. Unsupported Pd_3Sn was prepared using the same method and characterized by powder X-Ray diffraction. Pd_3Sn was found to be single-phase and isostructural to Pd metal with a face centred cubic unit cell and Sn atoms randomly substituting Pd atoms on their (0,0,0) crystal site.[12]

This paper focuses on the Pd-In system, specifically on compounds in which the ratio between Pd and In is approximately 3:1 (thereafter referred to as "Pd_3In") and 2 new catalysts "Pd_3In"/TiO_2 with "Pd_3In" compounds prepared at different temperatures. The reason behind the choice of In as co-metal in a Pd-based catalyst is the investigation and comparison of the catalytic properties with those of the previously reported Pd-Sn system. In fact, the Pd-In and Pd-Sn bimetallic systems have been reported and compared together in the literature.[13,14] Specifically, the compounds with stoichiometric ratio Pd:M = 3:1 can be found in both Pd-In and Pd-Sn systems. Pd_3Sn was reported to show a face-centred cubic unit cell, whereas "Pd_3In" has been reported as showing 2 polymorphs, both with a tetragonal unit cell. It has also been reported to

have a flexible Pd:In ratio and, in fact, Kohlman and Ritter reported $Pd_{3-x}In_{1+x}$ as a general formula.[14–18] In all cases, "Pd_3In" compounds were prepared via traditional high-temperature melting of Pd and In metals.

More recently, it was reported that the synthesis of metallic and bimetallic nanoparticles can be achieved by reacting metal salts in polyol solvents. The polyol solvent acts as reducing agent hence reducing the cations in the reagents to their metallic state. The polyol also act as surfactant, capping the particles and inhibiting their growth. This synthesis method relies on boiling points of the polyols hence requires lower temperature than the traditional method based on melting the metal reagents.[19,20]

There are a few reports in the literature on Pd–In combinations in various ratios, being used in catalysis applications.[21–23] However, in the current literature on the catalytic properties of Pd–In materials, little emphasis is placed on the Pd–In alloy or intermetallic phases present within the catalytically active material. These catalysts are often prepared by adding an indium precursor to a Pd catalyst as a "modifier".[22–25] This means that indium is often present as a separate phase in addition to Pd.[22,23]

In this work, we carried out the preparation of "Pd_3In" alloys and of the "Pd_3In"/TiO_2 catalyst via the low-temperature method based on the use of polyols; the same synthetic procedure was successfully employed in the preparation of Pd_3Sn and the catalysts Pd_3Sn /TiO_2 and Pd_3Sn /ZnO.[12,19,20]

We prepared two "Pd_3In" compounds using Ethylene Glycol (EG, boiling point = 197 °C) and Tetraethylene Glycol (TEG, boiling point = 314 °C) to achieve different synthesis temperatures.

In this way we stabilized two polymorphs with a cubic Pd-like unit cell and disordered substitution of In atoms on the Pd crystal site and, thanks to the use of different polyol solvents

with different boiling points, we obtained "Pd_3In" compounds with variable Pd:In ratios. We also obtained two "Pd_3In"/TiO_2 catalysts with higher selectivity than the model catalyst Pd/TiO_2.

2. Results and discussion

In this work, we aimed at the preparation and characterisation of nanocatalysts that show improved selectivity towards the semi-hydrogenation of alkyne, compared to the traditional Pd-based catalysts. We focussed on Pd-based nano alloys as catalytically active compounds, specifically on the Pd-In system in which the Pd/In ratio is approximately 3 ("Pd_3In"). This alloy has been reported to show two tetragonal polymorphs and variable Pd/In ratio ($Pd_{3-x}In_{1+x}$). The preparation of intermetallic compounds and alloys usually requires a reaction between two metals to occur at high temperature (often > 1000 °C).[26] More recently, it was reported that this can be achieved by mixing metal salts in polyol solvents with relatively high boiling points. The polyol solvents act as reducing agents, reducing the metals in the salts to their zero oxidation state then favouring the alloying process and, also, act as capping agents, favouring the growth of nanoparticles homogeneous in size and shape.[20]

The nanoalloys in this work were prepared via the polyol-based method, using ethylene glycol (EG, boiling point = 197 °C) and tetraethylene glycol (TEG, boiling point = 314 °C) to achieve different synthesis temperatures. The samples prepared in ethylene glycol and tetraethylene glycol will be referred to as EG and TEG respectively from here thereafter.

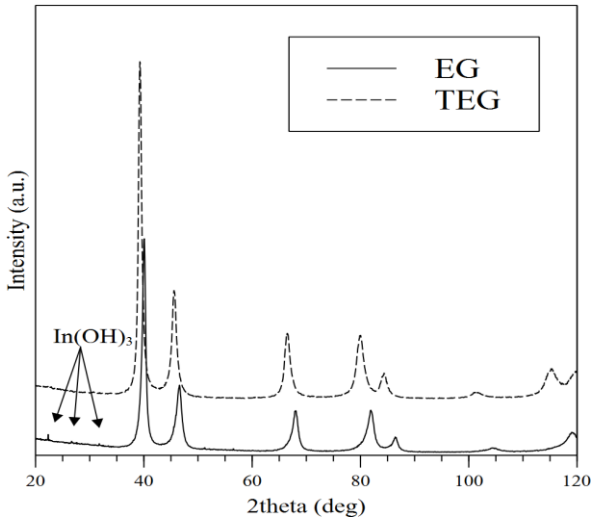

Figure 2. PXRD patterns of EG and TEG.

Powder X-Ray diffraction patterns were collected on the samples to determine their purity and crystal structures (Figure 2). The diffraction peaks could not be indexed using any of the tetragonal unit cells reported in the literature for the "Pd_3In" system, i.e. the $ZrAl_3$ type and the $TiAl_3$ type mainly. Instead, the peaks could be indexed using the cubic unit cell of Pd metal as a model.[11] Both "Pd_3In" compounds are single phase, however, the PXRD of the EG compounds shows some low intensity narrow peaks between 20 – 30 2 theta deg. and 50 – 60 2 theta deg. (figure 2). The nature of these low-intensity diffraction peaks is not clear, although they could be attributed to $In(OH)_3$, a possible by-product of the synthesis reaction. No peaks corresponding to either metallic In or indium oxide phases are observed, however the presence of these phases in amounts too small to be detected by PXRD cannot be ruled out entirely.

Both PXRD patterns of EG and TEG show the same diffraction peaks, however there is a notable shift towards higher 2theta angles for the "Pd_3In" compound prepared in EG. Calculations of the lattice parameters, deriving from Rietveld refinement of the PXRD data using the unit cell of Pd metal as a model (a = 3.859(3) Å) show that the unit cell of EG is smaller than the unit cell of TEG. (Table 1).

Table 1. The lattice parameters of the Pd–In materials calculated via Rietveld refinement of PXRD data.

"Pd_3In"	*a* (Å)
EG	3.8976(3)
TEG	3.9994(2)

Hellner and Laves reported the existence of the compound Pd_3In and classified its unit cell as face centred tetragonal.[27] Knight and Rhys prepared Pd_3In via melting ingots of the 2 metals and, via thermal analyses and microscopic examination, they found that the compound exists as tetragonal single phase for a range of 24.8 and 27 atomic % In content.[14] The Pd_3In phase was also reported by Harris et al to have a face centred tetragonal structure with a =4.0647 Å and c =3.7842 Å and (c/a=0.9310), in agreement with the values of a=4.06 Å and c=3.79 Å obtained previously by Knight and Rhys.[14,28] They also showed a PXRD pattern of a "crushed" or "deformed" Pd_3In phase, which shows a face-centred cubic type structure, observed mixed with the tetragonal phase within a narrow temperature range. Equation $a_{cubic} = (a_{tetr}^2 c_{tetr})^{\frac{1}{3}}$ was reported to calculate the a-spacing of a "hypothetical" FCC form of Pd_3In and would lead to a ~ 4 Å.[13] H. Okamoto reports 2 polymorphs, α and β Pd_3In. α Pd_3In contains between 74.5 and 75.5 atomic % Pd and is isostructural to Al_3Ti (*I4/mmm*). This structure type represents a superstructure of the cubic closest packing (Cu-type) with identical coordination numbers for all crystallographic sites. No structural or compositional data were given for the βPd_3In polymorph.[16]

Kohlman and Ritter prepared Pd_3In from the elements in evacuated sealed silica tubes via iodine-catalyzed synthesis at ~ 577 °C, a lower temperature than previously reported. Rietveld refinement was performed on PXRD and high-resolution neutron diffraction data.[17,18] X-Ray powder diffraction confirmed the $TiAl_3$ structure type proposed Okamoto for Pd_3In.[16] However, Rietveld refinement on neutron powder diffraction data reveals an In/Pd distributional disorder.

Therefore, the crystal structure of Pd_3In was described as a AuCu-type model instead (*P4/mmm*, a = 2.87224(4), c = 3.80079(7) Å), with mixed occupancy of one crystallographic site by 50% In and 50% Pd. Compositional variation, due to In/Pd distributional disorder, led to a general formula $Pd_{3-x}In_{1+x}$. Phase diagrams exhibited a homogeneity range from 24.8 to 26, and at temperatures above 1050 °C even up to 27 atomic % In. Unit cell volumes range from 126.132(5) $Å^3$ for the indium-rich to 125.474(8) $Å^3$ for the palladium-rich $Pd_{3-x}In_{1+x}$ phases.[17] Kohlman and Ritter, in a later paper reported that all the three tetragonal polymorphs for Pd_3In, represent closely related superstructures of a cubic closest packing as shown by a Bärnighausen symmetry tree.[18]

We have stabilised two cubic polymorphs of the $Pd_{3-x}In_{1+x}$ system, that have not been reported in the literature so far. It is impossible, though, at this stage to say whether the cubic unit cell reported here is primitive, implying an ordering of Pd and In atoms on different crystallographic sites or face centred cubic (FCC), implying disordered distribution of Pd and In atoms on the same (0,0,0) site. In fact, the "diagnostic" diffraction peaks that would allow a distinction between the 2 types of lattice and are seen in other Pd-metal compounds, cannot be seen for Pd-In compounds, as the 2 atoms show very similar x-ray diffraction factors. However, the unit cell of this cubic polymorph is more likely to be of the FCC type, as the low temperature of the synthetic approach tends to favour the creation of disordered structures, as shown by Kohlman et al.[18] Furthermore, it was reported that the polyol method can lead to metastable compounds, otherwise not accessible.[29,30]

The difference in lattice parameters between EG and TEG indicate different Pd:In ratios, specifically a higher content of In in TEG, given that the atomic radius of Pd is 1.37 Å and that of In is 1.66 Å.[31] The lattice parameter of EG is only slightly larger than that of Pd metal (a = 3.8973(3) Å, compared to a =3.859(3) Å[11]). EDX data, taken from several different areas,

indicate low level of In substitution, less than 13% at. X-Ray maps are shown in figure 3 and indicate an overall homogeneity in the elemental distribution. The apparent dishomogeneity in the X-Ray maps is a result of inhomogeneities in the thickness of the sample analysed and does not derive from real inhomogeneities in the element distribution (Figure 3). Hence EG is probably a cubic polymorph of "Pd_3In" with low In content, considering that the lattice parameter is not significantly higher than that of Pd metal and that part of the total In content must belong to the small impurity present, possibly $In(OH)_3$, as shown by the PXRD patterns (figure 2).

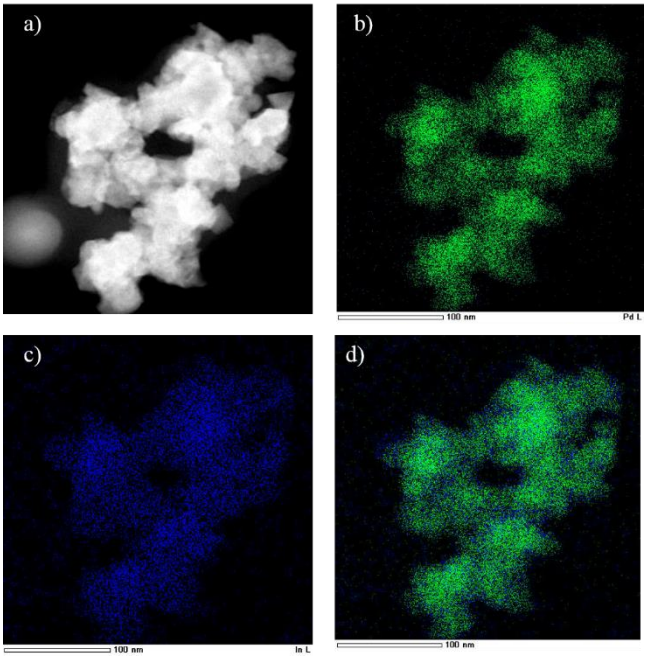

Figure 3. a) HAADF-STEM image of an agglomerate of EG; b) X-Ray map of the agglomerate in a) obtained using line L for Pd; c) X-Ray map of the agglomerate in a) obtained using line L for In; d) map obtained from the overlap of the individual maps in b) and c).

The lattice parameter of TEG is 0.1 Å larger than that of Pd metal. EDX data collected on several spots indicate an average Pd: In ≈ 75:25 ratio, in agreement with the ratio of the Pd and In salts used as reagents in the polyol reaction. The PXRD pattern does not show any diffraction peaks belonging to phases different from the Pd-like cubic phase (impurities), hence a single-phase

compound with chemical formula Pd_3In was obtained. The X-Ray maps show excellent homogeneity in the element distribution (Figure 4). Consequently, TEG can be considered a cubic polymorph of the Pd_3In compound, possibly the same "hypothetical" phase proposed by Harris et al.[13] HREM and Electron Diffraction confirm the cubic nature of the crystal structure (Figures 5 and 6).

In the ED pattern of TEG, four rings can be clearly distinguished (figure 5b). Starting from the most internal one, these rings correspond to the (111), (200), (220) and (311) lattice spacings of the cubic lattice of Pd.

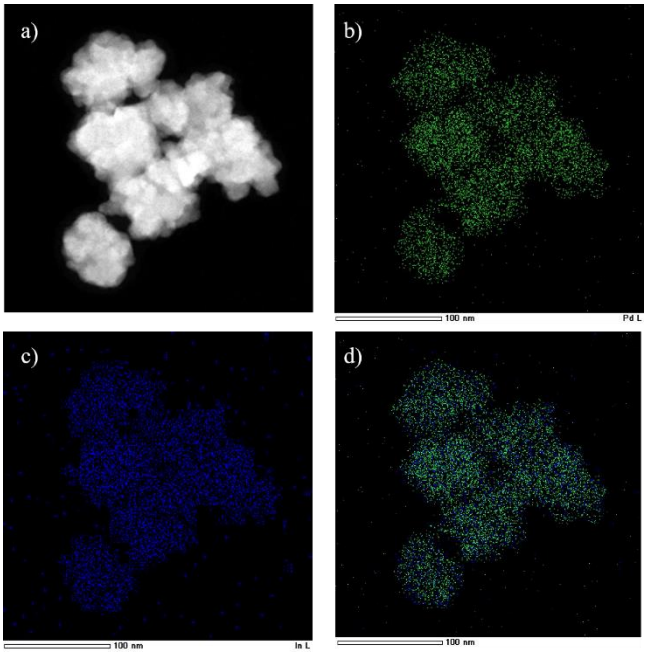

Figure 4. a) HAADF-STEM image of an agglomerate of TEG; b) X-Ray map of the agglomerate in a) obtained using line L for Pd; c) X-Ray map of the agglomerate in a) obtained using line L for In; d) map obtained from the overlap of the individual maps in b) and c).

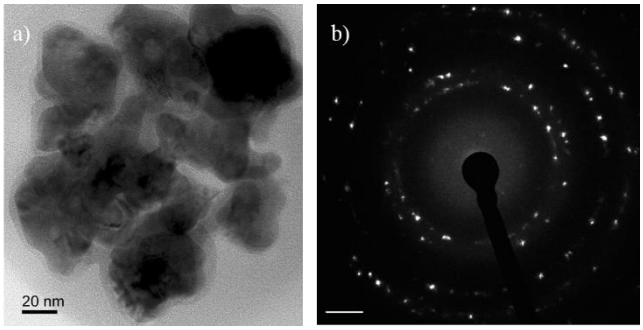

Figure 5. a) TEM image of a typical agglomerate of TEG particles and b) its ED ring pattern. Starting from the most internal one, these rings correspond to the (111), (200), (220) and (311) lattice spacings of the cubic lattice of Pd.

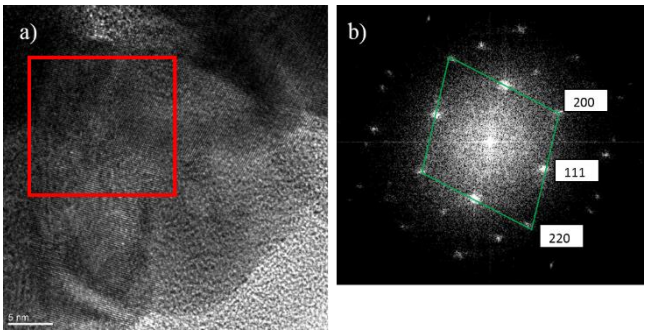

Figure 6. a) HREM of some particles and b) Fast Fourier Transform of the red squared region in a). The region contains a single particle lying in (110) projection. The lowest index reflections are reported.

Figure 6a shows the HREM image of some TEG nanoparticles. Fig 6b displays the Fourier transform of the red squared region in a), where the contribution of a single particle lying in a 110 type projection is highlighted by the green lozenge. The measured lattice spacings are perfectly coherent with the ones found in the ED pattern.

2.1 "Pd_3In"/TiO_2 Catalysts

"Pd_3In"/TiO_2 catalysts were prepared by adapting the same method and conditions used to prepare the "Pd_3In" catalytically active compounds so that the crystal structure of the supported and unsupported "Pd_3In" compounds could be compared. Polycrystalline support TiO_2 and the templating agent PVP were added to the reaction mixture of Pd and In acetates and the synthesis

carried out in the same conditions, using in both ethylene glycol and tetraethylene glycol as polyol solvents to vary the temperature. This also gave a convenient one-step reaction to prepare catalysts. The catalytic performance of the two "Pd_3In"/TiO_2 catalysts was assessed for the batch, liquid phase semi-hydrogenation of MBY. Pd/TiO_2 was also prepared and tested in the same condition for comparison. The two catalysts prepared in ethylene glycol and tetraethylene glycol will be named EG/TiO_2 and TEG/TiO_2 respectively from here thereafter.

PXRD was carried out on the catalysts, however no strong evidence of the presence of Pd/In within the catalyst is seen, as the pattern, predictably, is dominated by the TiO_2 support. This is due to the low percentage (< 2 wt%) of "Pd_3In" present in the catalysts as well as the very small particle size of the "Pd_3In" nanoparticles (< 10 nm) compared to that of the support (micron scale). The PXRD patterns show that the support is composed of mostly rutile-phase TiO_2, with approximately 3% of anatase. HRTEM was then carried out to obtain details of the crystal structure of the "Pd_3In" compounds, in order to understand if the same cubic structure is maintained when the compound is prepared in the presence of the support (TiO_2) and a templating agent (PVP).

10.1002/cctc.201900391

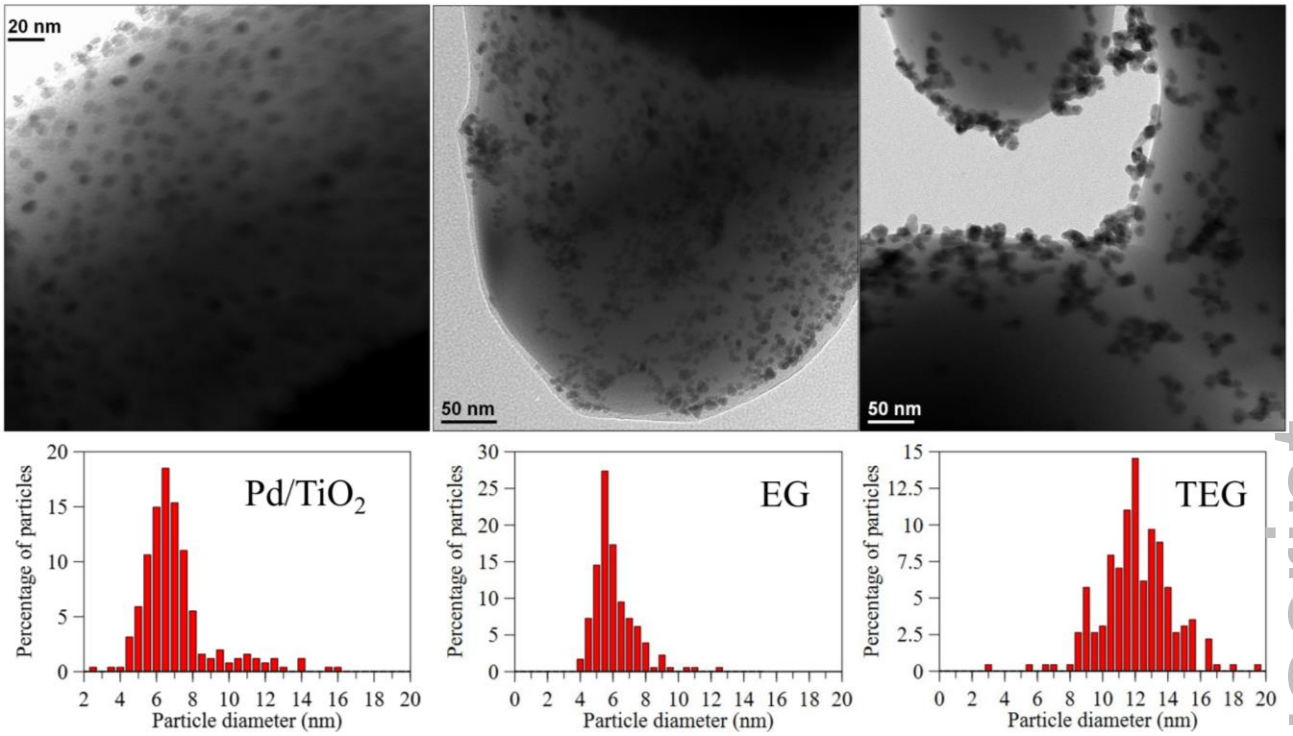

Figure 7. TEM images and the corresponding particle size distribution histograms of Pd/TiO_2, EG/TiO_2 and TEG/TiO_2.

The particle size distributions obtained from the TEM micrographs (examples shown in Figure 7) show that the materials prepared in TEG have larger particle diameter compared to those prepared in EG (mean particle size = 5.8(±1.3) nm in EG/TiO_2 compared to 11.8(±2.2) nm in TEG/TiO_2). The mean particle diameter of EG/TiO_2 is also slightly lower than that seen in Pd/TiO_2 (6.8(±2) nm), which mirrors observations made in our previous work in which Pd_3Sn catalysts prepared using EG showed lower particle size than Pd catalysts prepared in the same way.[12] The mean particle diameter for TEG/TiO_2 is almost twice larger than that of EG/TiO_2 and Pd/TiO_2 and is well outside of their standard deviations.

10.1002/cctc.201900391

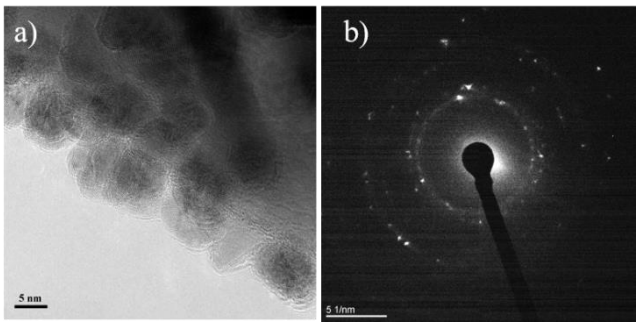

Figure 8. a) HRTEM micrograph and b) ED patterns for EG/TiO_2.

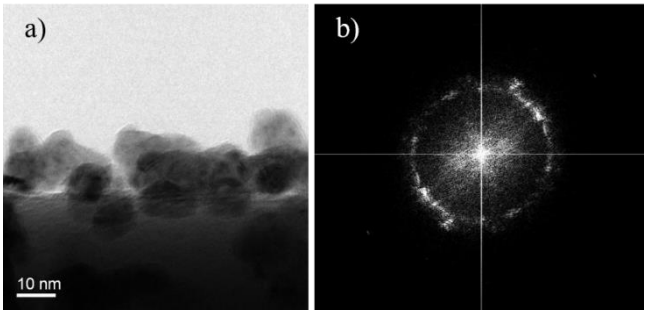

Figure 9. a) HREM images of TEG/TiO_2; b) Fast Fourier Transform (FFT) for TEG/TiO_2.

HRTEM images show that the nanoparticles of the catalytically active compound EG are approximately spherical, with homogeneous size distribution (Figure 8a). The nanoparticles of the catalytically active compound TEG appear to show more agglomeration and, in general, a more irregular shape (Figure 9a). Several nanoparticles are observed that are partially fused together. This may be due to the higher temperature at which each TEG reaches reflux (314 °C in TEG compared to 197 °C in EG), which can cause particle growth and sintering. Decomposition of the capping agent, PVP, may have also occurred at the higher temperature, which can affect particle size since the presence of PVP restricts nanoparticle growth.

Table 2. *d*-spacings of EG/TiO_2, TEG/TiO_2 calculated from FFT, and Pd from ref. [28]

EG/TiO_2 *d*-spacings (nm)	TEG/TiO_2 *d*-spacings (nm)	Pd *d*-spacings[28] (nm)	Reflection
0.22	0.23	0.25	111
0.19	0.20	0.19	200
0.13	0.14	0.13	220
0.12	-	0.12	311

In both cases, the *d*-spacings estimated by fast Fourier Transform (FFT) (Table 2) are comparable with those reported for Pd metal.[28] This is similar to observations made for unsupported EG and TEG, in which PXRD shows a phase similar to Pd metal. Hence, the available evidence suggests that the unsupported and the supported "Pd_3In" materials show the same crystal structure.

STEM-HAADF image and X-ray maps were collected from the same areas of the EG/TiO_2 and TEG/TiO_2 samples and are shown in Figures 10 to 12. X-ray maps show that the elements Pd and In are distributed homogeneously throughout all nanoparticles in both cases, providing good evidence that Pd/In form a single, homogeneous alloy in each catalyst. Furthermore, Ti (red) is shown exclusively in the support, with nanoparticles not in contact with the support showing no Ti content, hence strengthening the notion that no reaction or strong metal-support interaction (SMSI) has occurred between Pd–In nanoparticles and the TiO_2 support. EDX measurements find almost everywhere the nominal composition for EG/TiO_2 (Pd:In ~ 75:25) but a higher content of In in TEG/TiO_2 (Pd:In ~ 66:34). These findings are in contrast with the EDX data and the X-Ray maps obtained from the EG and TEG pure compounds. In fact the In content in EG was found not to be above 13% at but a nominal Pd:In ≈ 75:25 ratio was found for TEG in many area of the samples. It appears that the presence of the support in the reaction pot does not influence the crystal phase but does influence the element ratio of the alloy.

10.1002/cctc.201900391

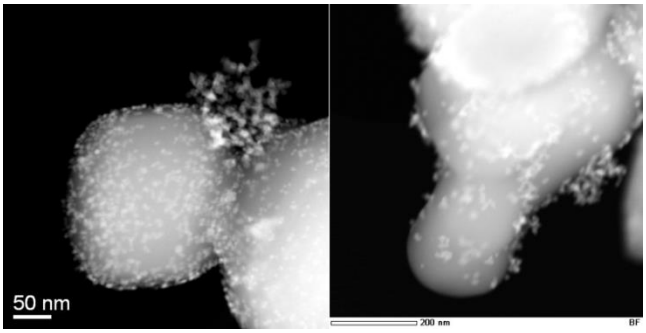

Figure 10. STEM-HAADF micrographs of EG/TiO_2 (left) and TEG/TiO_2 (right).

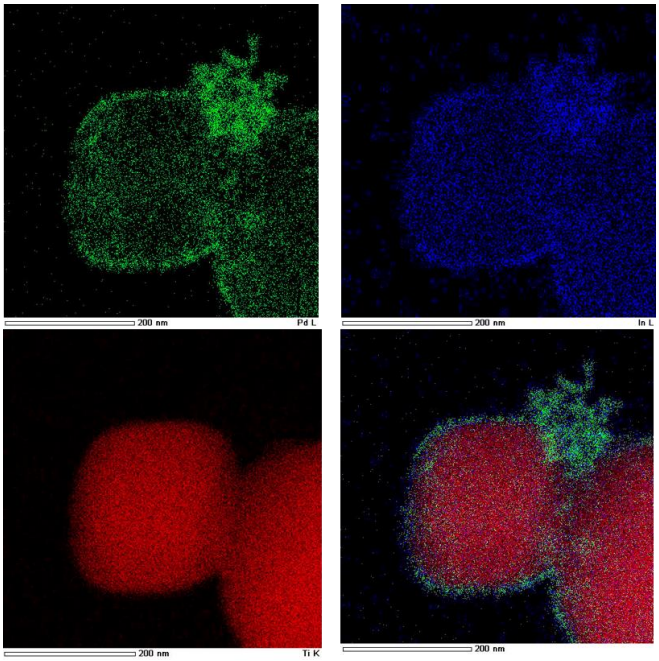

Figure 11. X-ray maps of EG/TiO_2 referred to agglomerate shown in figure 10 and showing the spatial distribution of Pd (green), In (blue), Ti (red). and the combination of Pd and In, and Ti.

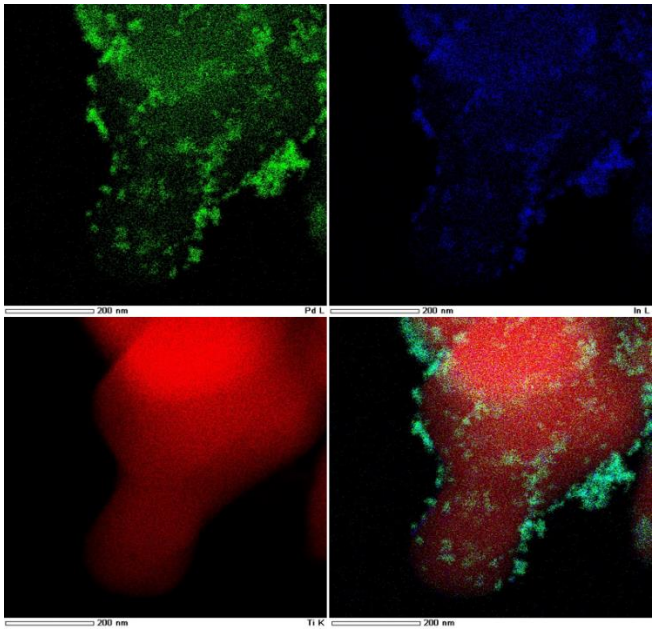

Figure 12. X-Ray maps of TEG/TiO_2 referred to agglomerate in figure 10 (right) and showing the spatial distribution of Pd (green), In (blue), Ti (red), and the combination of Pd, In, and Ti.

2.2 Catalytic Performance

To screen the catalytic performance of EG/TiO_2 and TEG/TiO_2, a liquid phase batch hydrogenation of MBY was carried out using each of the catalysts. The reaction scheme is shown in Figure 1 and the reaction profiles using each catalyst are shown in Figure 13. For each of the Pd–In catalysts, the hydrogenation reaction proceeds as expected for a Pd-catalysed hydrogenation of an alkyne. Firstly, MBE is produced via the hydrogenation of MBY. Very little MBA is formed in comparison to MBE until almost full conversion of MBY into MBE, after which only MBA is produced via the hydrogenation of MBE. This shows that the reaction proceeds mostly by successive stepwise hydrogenation; first, MBE is produced by semi-hydrogenation of MBY (Figure 1, a), then MBA is produced by hydrogenation of MBE in a separate step (Figure 1, b). The full hydrogenation of MBY into MBA (Figure 1, c) is avoided. This reaction behaviour is expected for Pd-based catalysts as alkynes (MBY) are known to be preferentially adsorbed to the surface of Pd compared to alkene bonds (MBE).[4,5]

The carbon balance (the total moles of MBY, MBE and MBA) does not decrease over time during any of the hydrogenation reactions, indicating no other products are formed by dimerization reactions, etc., as sometimes observed in the semi-hydrogenation of MBY.[32–34]

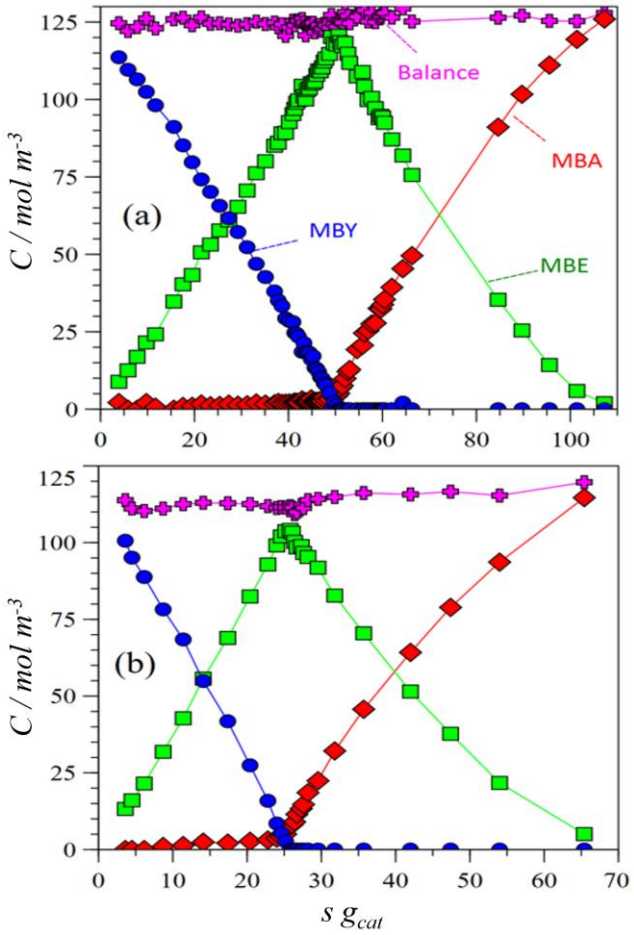

Figure 13. Experimental data showing the concentrations of MBY (blue), MBE (green), MBA (red) and balance (purple) over time (seconds per gram of catalyst) during a semi-hydrogenation reaction at 308 K, 1 atm. H_2 pressure, 0.12 M solution of MBY in hexane. The catalysts are: (a) EG/TiO_2 and (b) TEG/TiO_2.

The differences between the performance of each catalyst can be seen with their activity, (*A*) normalised per mole of Pd present in the catalyst (Figure 14), i.e. how quickly the hydrogenation reaction takes place per catalyst amount, and the selectivity towards MBE, i.e. how much MBE is produced compared to MBA (and any other reaction products) up to full conversion of MBY.

TEG shows higher activities than Pd/TiO_2 while EG shows slightly lower activity (0.30 s^{-1} compared to 0.37 s^{-1} for Pd/TiO_2).[12] It is difficult to say why EG/TiO_2 has lower activity, especially considering that according to EDX measurements EG contains more Pd than TEG.

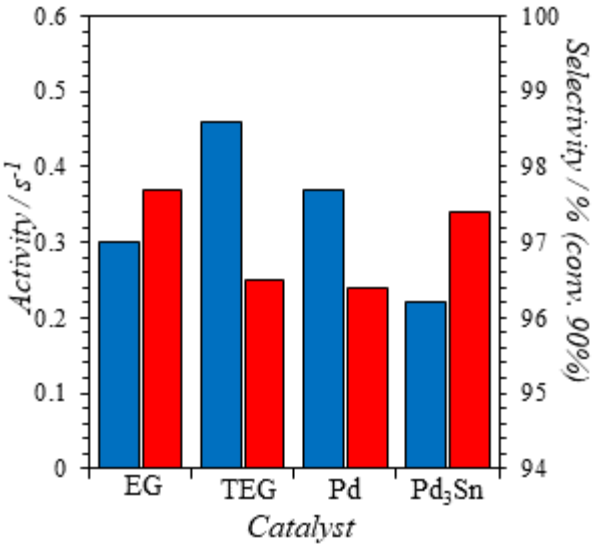

Figure 14. Graph of activities (blue) and selectivities (red) at different MBY conversions ($S_{MBE,90}$ (%)) in the semi-hydrogenation of MBY at 308 K, 1 atm. H_2 pressure, 0.12 M solution of MBY in hexane of different Pd-In catalysts, Pd/TiO_2 and Pd_3Sn/TiO_2.[12]

It is apparent that both EG/TiO_2 and TEG/TiO_2 show higher selectivity than Pd/TiO_2 (Figures 14 and 15). The catalyst activities and selectivities are also compared to Pd_3Sn/TiO_2, which was prepared following the same procedure as EG/TiO_2 except using tin acetate as co-metal precursor instead of Indium acetate.[12] EG/TiO_2 also shows comparable (slightly higher) selectivity than Pd_3Sn/TiO_2, however the activity of EG/TiO_2 is increased by around one-third in comparison. Between the two "Pd_3In" catalysts, EG/TiO_2 shows higher selectivity than TEG/TiO_2. The reason for this is not obvious and may be a combination of several factors such as, higher In content in TEG/TiO_2 possibly impacting on the selectivity and/or, the fact that the nanoparticles of EG/TiO_2 may be more "dispersed" than those of TEG/TiO_2, as shown by HREM images (Figures 7–9).

S_{MBE} for TEG/TiO_2 is slightly lower at all stages of the reaction compared to EG/TiO_2 and Pd_3Sn/TiO_2, however both catalysts maintain higher S_{MBE} compared to Pd/TiO_2.

The higher selectivity shown by both EG/TiO_2 and TEG/TiO_2 catalysts indicates that the addition of a second metal, In in this case, to form an alloy with Pd does enhance the catalytic properties of Pd metal towards MBE. However, the metal and co-metal ratio seem to be a factor in determining the catalytic performance.

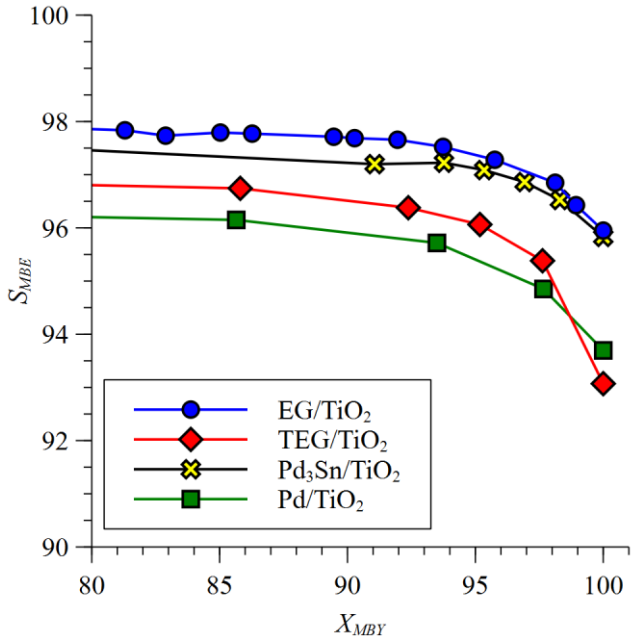

Figure 15. Selectivity towards MBE (S_{MBE}) as a function of MBY conversion (X_{MBY}) during the semi-hydrogenation of MBY at 308 K, 1 atm. H_2 pressure, 0.12 M solution of MBY in hexane using different Pd-In catalysts, Pd_3Sn/TiO_2 and Pd/TiO_2.

3. Experimental

3.1 Materials

The metal precursors used in the catalyst preparation were palladium(II) acetylacetonate (99%, Aldrich) and indium(III) acetate (99.99%, Aldrich). Titanium(IV) oxide, rutile (≥99.0%, Aldrich) was used as support material and polyvinylpirrolidone (average mol. Wt. 40'000 g mol^-

[1], Sigma-Aldrich) was used as a capping agent. Acetone (laboratory reagent grade, Fischer Chemical), ethanediol (laboratory reagent grade, Fischer Chemical), n-hexane (GPR grade, VWR Chemicals) and deionised water were used as solvents without any pre-treatment. For the hydrogenation reactions, butan-1-ol (analytical reagent grade, Fisher Scientific) was used as internal standard for GC analysis. All chemicals were used as purchased.

3.2 Preparation of Pd–In Particles and catalysts

The method used for the preparation of the Pd-In particles and catalysts is the same as described in previous work for the synthesis of Pd_3Sn materials[12], except using indium(III) acetate rather than tin(II) acetate, and either ethylene glycol (EG) or tetraethylene glycol (TEG) as the polyol solvent. The method is adapted from a polyol method used by Cable and Shaak for the preparation of Pt_3Sn.[35]

For the preparation of Pd-In particles, appropriate stoichiometric amounts of the metal precursors, palladium(II) acetylacetonoate and indium(III) acetate, each in 100 mL of either ethylene glycol or tetraethylene glycol were combined and heated at reflux (470 K in EG, 587 K in TEG) for 1 hour under nitrogen gas flow. No capping agent or support was used for the synthesis of the Pd-In particles to allow for analysis of the catalytically active compound.

For the synthesis of the catalysts, a "one-pot" synthesis procedure was used in which TiO_2 support and the PVP capping agent (10 mol% of total Pd and In) were added alongside the Pd and In precursor solutions before heating at reflux. The amount of the support used was calculated to achieve 2 wt% Pd loading.

Once cool, Pd-In particles and catalysts were obtained by centrifugation at 3000 rpm, washing with deionised water and acetone (3 × 30 mL each) and dried at 353 K in air for 1 h.

3.3 Characterisation of the Catalytically Active Compounds

Powder X-ray diffraction (PXRD) was carried out using a PANalytical Empyrean X-ray diffractometer using monochromatic Cu Kα1 radiation and line PIXcel detector. Results were recorded and analysed using the instrument's built-in software.

The PXRD for unsupported Pd–In materials was carried out by scanning in the 2θ range of 10-140°, step size 0.05° and step time 1.0 seconds. For these measurements, a fixed divergence slit was used with slit size 0.5°.

PXRD for the Pd-In catalysts was carried out by scanning in the 2θ range of 5-120°, step size 0.02° and step time 1.0 seconds. The instrument's built-in automatic divergence slit was used. However, the PXRD patterns were dominated by the TiO_2 support, and no peaks arising from Pd/In compounds could be observed.

Rietveld refinement of PXRD data was performed to confirm the cubic crystal structure, via the software GSAS.[36,37] The model used was the cubic unit cell of Pd metal (a = 3.859(3) Å,[11] with In and Pd occupying the same site (x=0; y=0; z=0) with occupancies fixed at 75% for Pd and 25 % for In and the lattice parameter replaced with the one calculated from indexing of the PXRD data using the PANalytical HighScore Plus software. The peak profile was modelled with the software CMPR and the values for U, V, W, Gaussian (GP) and Lorentzian (LX) size broadening substituted in the input file.[38]

Analytical and conventional transmission electron microscopy (TEM) studies were performed in a high-resolution (HR) (0.18 nm) field emission JEOL 2200FS microscope operating at 200 kV, equipped with an in-column Ω energy filter, two High-Angle Annular Dark Field (HAADF) detectors for the so-called 'Z-contrast' imaging and an Energy Dispersive X-ray Spectrometer (EDX) for collecting X-ray spectra and X-ray mapping. The nanostructures were dispersed on holey carbon grids for the observation.

3.4 Hydrogenation Reaction

For the semi-hydrogenation of MBY catalysed by the Pd and Pd-In catalysts, freshly-prepared catalysts (between 5 and 50 mg, depending on the activity of the catalyst) and a hexane solution (100 mL) containing 0.741 g (10 mmol) of butan-1-ol used as an internal standard were transferred into a 250 mL 3-neck round bottom flask fitted with a silicone rubber septum, thermometer and reflux condenser. A Schlenk line was connected through the top of the condenser to enable alternation between nitrogen gas, hydrogen gas, and vacuum. The contents of the flask were stirred at 1100 rpm and heated to 308 K. Air from the reactor and the solvent was removed purging the reactor 3 times with nitrogen gas – the pressure was slowly decreased until the solvent started to boil, and the reactor was filled with nitrogen gas quickly. Nitrogen gas was then similarly substituted by hydrogen gas, purging the reactor 3 times. The contents were left stirring under hydrogen atmosphere (ambient pressure) for approximately 30 min to ensure the solvent and catalyst were saturated with hydrogen, and that no leak was present in the system (the hydrogen consumption was measured by a 300 mL gas burette). The reaction was started by quickly injecting 1.00 g MBY using a syringe through the septum. Aliquots of approximately 150 μL were taken at regular intervals with the increased sampling rate when the reaction approached 100% conversion (estimated using hydrogen consumption). Analysis of the products was performed using a Varian 430 gas chromatograph equipped with a 30 m Stabilwax® capillary column (Restek). A series of experiments with various stirring rates and catalyst amounts confirmed the absence of external mass transfer limitations. Conversion of MBY (X_{MBY}) and selectivity to MBE ($S_{MBE,x}$) at different levels of conversion were calculated using Eqs. (1)–(2), where C_{MBY}, C_{MBE}, C_{MBA} and C_x are the concentrations of MBY, MBE, MBA and the concentrations at x% MBY conversion, respectively. These formulae imply that no components other than MBY, MBE and MBA were obtained, which was confirmed by the carbon balance ($C_{MBY} + C_{MBE} + C_{MBA}$) for all reactions of 100 ± 2%.

$$X_{MBY} = \frac{C_{MBE} + C_{MBA}}{C_{MBY} + C_{MBE} + C_{MBA}} \quad (1)$$

$$S_{MBE,x} = \frac{100 \times C^{X}_{MBE}}{C^{X}_{MBY} + C^{X}_{MBE} + C^{X}_{MBA}} \quad (2)$$

The activity of the catalysts was characterised per mol. of Pd (*A*) using the average MBY consumption rate in 0-80% MBY conversion interval as in Equation (4), where X^{80}_{MBY} is the MBY conversion close to 80% occurred during the reaction time of t^{80}_{MBY}, C^{80}_{MBY} is the initial MBY concentration, V_{sol} is the solution volume, m_{cat} is the catalyst mass taken with Pd content of ω_{Pd}, and M_{Pd} is the molar mass of Pd.

$$A = \frac{1 - X^{80}_{MBY}}{t^{80}_{MBY}} \frac{C^{0}_{MBY} V_{sol} M_{Pd}}{m_{cat} \omega_{Pd}} \quad (3)$$

4. Conclusions

We prepared and characterised "Pd_3In" ($Pd_{3-x}In_{1+x}$)/TiO_2 nanocatalysts, which show both improved activity and selectivity compared to pure Pd catalysts, towards the liquid phase semi-hydrogenation of 2-methyl-3-butyn-2-ol (MBY) to 2-methyl-3-buten-2-ol (MBE). Conventionally, alloys are prepared via melting of the metals at temperature above 1000 °C, however, we used a polyol-based method, which relies on the boiling point of polyol solvents to reach temperature. Specifically, we prepared two catalytically active alloys, "Pd_3In" ($Pd_{3-x}In_{1+x}$),

and their corresponding catalysts, "Pd_3In" ($Pd_{3-x}In_{1+x}$)/TiO_2, in the same conditions, using ethylene glycol (reaction temperature 194 °C) and tetraethylene glycol (reaction temperature 345 °C) as solvents.

We were able to prepare two single-phase "Pd_3In" ($Pd_{3-x}In_{1+x}$) compounds. "Pd_3In" ($Pd_{3-x}In_{1+x}$) compounds have been reported to show two polymorphs with tetragonal unit cells. However, PXRD showed that both our compounds showed a Pd-like cubic structure, indicating that the use of lower synthesis temperature allowed for the stabilisation of new polymorphs. HREM confirms that the same cubic symmetry is shown by the "Pd_3In" ($Pd_{3-x}In_{1+x}$) compounds also when prepared as catalysts, i.e. in the presence of the TiO_2 support and the PVP templating agent. However, the extra components in the reaction mixture seem to have an effect on the Pd:In ratio, which is different in the supported and unsupported "Pd_3In" ($Pd_{3-x}In_{1+x}$) compounds. In this work, the variation of the element ratio did not influence the crystal structure of the catalytically active compounds, due to the structural flexibility and the alloy nature of the compound itself. However, a change in metal ratio caused by the presence of the support in the preparation routine for the catalyst may become crucial for catalysts based on intermetallic compounds with fixed elements ratio.

Conflicts of interest

There are no conflicts to declare.

Acknowledgements

This work was carried out under an EU funded FP 7 project: Microwave, Acoustic and Plasma Synthesis, Project Number FP70NMP-2012-SMALL-6.

We wish to acknowledge the use of the EPSRC funded National Chemical Database Service hosted by the Royal Society of Chemistry.

We are grateful to Ann Lowry and Bob Knight for TEM and ICP analyses, respectively.

Graphical abstract

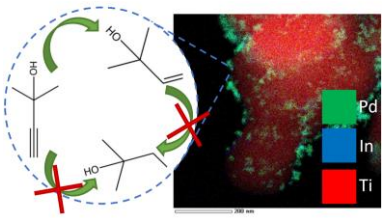

New "Pd_3In"/TiO_2 nanocatalysts show improved performance towards the liquid phase semi-hydrogenation of 2-methyl-3-butyn-2-ol (MBY). The catalysts are prepared via a one-step one-pot synthetic method and are based on two new cubic polymorphs of "Pd_3In", with tunable Pd/In ratios, thanks to the use of different solvents/temperatures during the synthesis process. PXRD, HREM and X-Ray maps show that the cubic polymorphs are formed with or without the support, however, the support seems to influence the Pd/In ratio.

Keywords: Cubic polymorphs; Pd/In alloys; Pd_3In catalysts; selective hydrogenation; tunable compositions of alloys.

References

1 W. Bonrath, J. Medlock, J. Schutz, B. Wustenberg and T. Netscher, *Hydrogenation in the Vitamins and Fine Chemicals Industry – An Overview*, InTech, 2012.

2 W. Bonrath, M. Eggersdorfer and T. Netscher, *Catal. Today*, 2007, **121**, 45–57.

3 M. Eggersdorfer, D. Laudert, U. Létinois, T. McClymont, J. Medlock, T. Netscher and W. Bonrath, *Angew. Chem. Int. Ed. Engl.*, 2012, **51**, 12960–12990.

4 G. C. Bond, D. A. Dowden and N. Mackenzie, *Trans. Faraday Soc.*, 1958, **54**, 1537.

5 Á. Molnár, A. Sárkány and M. Varga, *J. Mol. Catal. A Chem.*, 2001, **173**, 185–221.

6 H. Lindlar, *Helv. Chim. Acta*, 1952, **35**, 446–450.

7 J. A. Anderson, J. Mellor and R. P. K. Wells, *J. Catal.*, 2009, **261**, 208–216.

8 B. Coq and F. Figueras, *J. Mol. Catal. A Chem.*, 2001, **173**, 117–134.

9 A. Borodziński and G. C. Bond, *Catal. Rev.*, 2008, **50**, 379–469.

10 W. Palczewska, A. Jabłonski, Z. Kaszkur, G. Zuba and J. Wernisch, *J. Mol. Catal.*, 1984, **25**, 307–316.

11 W. P. Davey, *Phys. Rev.*, 1925, **25**, 753–761.

12 S. K. Johnston, N. Cherkasov, E. Pérez-Barrado, A. Aho, D. Y. Murzin, A. O. Ibhadon and M. G. Francesconi, *Appl. Catal. A Gen.*, 2017, **544**, 40–45.

13 I. R. Harris, M. Norman and a. W. Bryant, *J. Less Common Met.*, 1968, **16**, 427–440.

14 J. R. Knight and D. W. Rhys, *J. Less Common Met.*, 1959, **1**, 292–303.

15 I. R. Harris and M. Cordey-Hayes, *J. Less Common Met.*, 1968, **6**, 223–232.

16 H. Okamoto, *J. Phase Equilibria*, 2003, **24**, 481–481.

17 H. Kohlmann and C. Ritter, *Z. Naturforsch.*, 2007, **62**, 929–934.

18 H. Kohlmann and C. Ritter, *Z. für Anorg. und Allg. Chemie*, 2009, **635**, 1573–1579.

19 F. Fievet, J. P. Lagier and M. Figlarz, *MRS Bull.*, 1989, **14**, 29–34.

20 R. E. Cable and R. E. Schaak, *Chem. Mater.*, 2005, **17**, 6835–6841.

21 I. Witońska, S. Karski, J. Rogowski and N. Krawczyk, *J. Mol. Catal. A Chem.*, 2008, **287**, 87–94.

22 M. G. Davie, K. Shih, F. A. Pacheco, J. O. Leckie and M. Reinhard, *Environ. Sci. Technol.*, 2008, **42**, 3040–3046.

23 J. Zhao, W. Li and D. Fang, *RSC Adv.*, 2015, **5**, 42861–42868.

24 B. P. Chaplin, J. R. Shapley and C. J. Werth, *Catal. Letters*, 2009, **130**, 56–62.

25 R. Zhang, D. Shuai, K. A. Guy, J. R. Shapley, T. J. Strathmann and C. J. Werth, *ChemCatChem*, 2013, **5**, 313–321.

26 M. G. Kanatzidis, R. Pottgen and W. Jeitschko, *Angew. Chem. Int. Ed. Engl.*, 2005, **44**, 6996–7023.

27 E. Hellner and F. Laves, *Z. Naturforsch.*, 1947, **2**, 177–184.

28 I. R. Harris and M. Norman, *J. Less-Common Met.*, 1968, **15**, 285–298.

29 B. M. Leonard, N. S. P. Bhuvanesh and R. E. Schaak, *J. Am. Chem. Soc.*, 2005, **127**, 7326–7327.

30 Y. Zhao, Y. Zhang, H. Zhu, G. C. Hadjipanayis and J. Q. Xiao, *J. Am. Chem. Soc.*, 2004, **126**, 6874–6875.

31 L. Pauling, *J. Am. Chem. Soc.*, 1947, **69**, 542–553.

32 M. Crespo-Quesada, M. Grasemann, N. Semagina, A. Renken and L. Kiwi-Minsker, *Catal. Today*, 2009, **147**, 247–254.

33 M. Crespo-Quesada, F. Cárdenas-Lizana, A. L. Dessimoz and L. Kiwi-Minsker, *ACS Catal.*, 2012, **2**, 1773–1786.

34 E. V. Rebrov, E. A. Klinger, A. Berenguer-Murcia, E. M. Sulman and J. C. Schouten, *Org. Process Res. Dev.*, 2009, **13**, 991–998.

35 R. E. Cable and R. E. Schaak, *J. Am. Chem. Soc.*, 2006, **128**, 9588–9589.

36 B. H. Toby, *J. Appl. Crystallogr.*, 2001, **34**, 210–213.

37 R. B. Von Dreele and A. C. Larson, *General structure analysis system (GSAS)*, 2004.

38 B. H. Toby, *J. Appl. Crystallogr.*, 2005, **38**, 1040–1041.